Determination of adsorption capacities of N_2 and CO_2 on commercial activated carbon and adsorption isotherm models

Hazal Öztan[1,2*], and *Duygu* Uysal[1]

[1] Gazi University, Faculty of Engineering, Chemical Engineering Department, 06570 Maltepe, Ankara, Turkey
[2] Gazi University, Graduate School of Natural and Applied Sciences, 06500 Teknikokullar, Ankara, Turkey

Abstract. In today's technologies of gas purification systems, adsorption processes offer more advantages than traditional processes (amine absorption and cryogenic distillation). Thanks to advantages such as high efficiency, low energy consumption and ease of operation, the adsorption process plays an important role in today's natural gas purification and carbon capturing processes. In order to bring natural gas to the usage standards and to ensure carbon capture in the emission sources (coal mines, landfills, agricultural activities, etc.) that emit CO_2-CH_4 as a result of human activities, it is extremely important to purify impurities such as CO_2 and N_2, which are highly present in the gas mixture. In the study, the adsorption of N_2 and CO_2 gases on activated carbon and the effect of pressure and temperature on adsorption were examined. The operating conditions pressure range was 1-6 bar and temperatures below room temperature. Experimental studies were carried out in laboratory scale adsorption cell system. As a result of the studies, it was determined that the adsorption capacity of activated carbon N_2 and CO_2 increased with pressure. N_2 adsorption capacities were determined between 0.4-7.8 mmol/g and CO_2 adsorption capacities were determined in the range of 2.7-7.4 mmol/g. In addition, Langmuir and Freundlich isotherm models were created, model parameters were examined and the adsorption behaviour of activated carbon for CO_2 and N_2 gases was obtained.

Keywords: adsorption; activated carbon; coal bed methane; PSA; adsorption isotherms.

1 Introduction

The increase in energy demand and the depletion of fossil fuel reserves faster than predicted are the biggest problem of today's energy economy. In addition to this economic-oriented problem, the biggest environmental problem of conventional power generation systems is greenhouse gas emissions. Flue gas emissions of conventional systems are the main component of global CO_2 emissions, as of February 2023, according to data from the Mauna Loa observatory, its concentration in the atmosphere is 420.57 ppm [1]. However, CH_4 gas which ranks second among antropogenic greenhouse gas emissions, is 28 times more effective than CO_2, and its concentration in the atmosphere exceeded 1893 ppb in January 2020 [2, 3]. The sources of CH_4 emissions as a result of human activities are coal mines, landfills, livestock fattening activities and agriculture. However, CH_4 gas is an important source of fossil fuels. The fact that it emits less CO_2 per unit of energy when burned compared to coal and petroleum products has led to its being considered a cleaner energy source and sources containing CH_4 for its production to be at the forefront of national energy strategies [4]. For this reason, the purification of the streams in coal mines, which have CH_4 emission, and the production of natural gas suitable for use is an important subject of today's researches.

The methane in the gas stream in coal mines is called coal bed methane. It is a type of unconventional natural gas, and the content of the gas stream is highly dependent on the geological characteristics and location of the coal bed. Coal bed methane, while being complex and heterogeneous, basically contains CH_4 and largely CO_2 and N_2. Depending on the location of the coal mine, H_2O and various hydrocarbon compounds may also present [5, 6]. Due to the high demand for natural gas, coal bed methane containing CH_4 must be retained and purified by appropriate processes. In order to CH_4 to be supplied to pipelines, the gases CO_2 and N_2 in its content must be removed. If the sales gas limit values are exceeded, the natural gas stream is purified by a process called sweetening [7]. The content of CO_2 and N_2 reduces the calorific value of the gas, and CO_2 is an acidic gas and also causes corrosion in pipelines. Therefore, impurities in the gas stream are undesirable.

Natural gas purification technologies include amine absorption, cryogenic distillation, membrane systems and adsorption processes. In today's technologies, CO_2 removal with amine absorption is carried out in large-scale facilities with high energy demand in amine/water and regeneration. Likewise, under cryogenic operating conditions (80bar, -170°C) can be separated from natural gas by N_2 with a very high energy requirement. In membrane systems and natural gas purification, the fact that membrane production is very costly as a result of system-specific material needs and gas molecule-specific optimization conditions is a big problem of these systems. In the

adsorption process, pressure swing adsorption (PSA-pressure swing adsorption) systems are the preferred in laboratory and pilot scale systems for CO_2 capture in the flue gas outlets of steam reformer output gas, natural gas and traditional fossil fuel power generation systems. It has advantages over conventional systems (absorption and cryogenic distillation) such as low energy consumption, high efficiency, being environmentally friendly and simplicity [7, 8].

The functioning of PSA systems consists of two basic stages. The first stage is the adsorption of the adsorbate gas on the solid adsorbent until it becomes saturated. The second stage is the desorption/release of the adsorbted component and its preparation for the next cycle. The heart of the PSA system is the selection of an adsorbent with high selectivity to the adsorbate gas, as it is the most important determinant of PSA efficiency. This is because the achievement of a high separation/purification efficiency depends on the affinity of the adsorbate gas depending on its molecular properties and the electrical properties between gas and the adsorbent [9]. There are lots of adsorbents that are manufactured with some commercial names in zeolite groups such as 13X zeolite, 4A, 5A, Silicalite, Hβ so on. Also, carbon molecular sieves group has CMS-3K as a commercial adsorbent. In the literature, metal organic frameworks (MOFs) are presented Cu-MOF, MIL-101, DD3R, ETS-4 MOF-508b as an adsorbent for purification studies. Especially activated carbons are the most used adsorbents in industry and literature, and also this group has many commercial varieties like Xtrusorb A754, Norit-RB2, Norit-RB3, BPL, and F-400. Although many natural and synthetic adsorbent classes are included in the literature in the purification of natural gas, activated carbons, carbon molecular sieves, zeolites and metal organic frameworks (MOF) are the most preferred material groups due to their low energy requirements in regeneration. The fact that activated carbons have a high surface area, well-developed pore structure, high adsorption capacity at high pressure values, strong-durable structure (skeleton) and also that they can be easily obtained from cheap agricultural wastes allow them to be used effectively as adsorbents. In addition, the fact that the functional groups or organic bonds they have can be changed by pre-treatment for further expands their use, contributing to the improvement of surface/electrical properties [10, 11, 12].

The mechanisms of adsorption are basically a process by which the adsorbate gas attaches physically to a solid-porous adsorbent with weak Van der Waals forces, and chemically thanks to chemical bonds. For adsorption applications, adsorption isotherm is an important thermodynamic equilibrium relationship that indicates the amount of gas adsorbed on an adsorbent as a function of pressure at a constant temperature. Determining how adsorption mechanisms occur is of great importance for designing adsorption systems. Many mathematical adsorption models are used to determine adsorption mechanisms and equilibrium capacities. Modeling of adsorption data with isoterm models is the most appropriate and widely used method. Furthermore, adsorption isotherm models are also helpful in acquiring knowledge about adsorption capacity, which is important in evaluating the performance of adsorbents. The most commonly used isotherm models are Langmuir, Freundlich, Sips, Toth, Temkin, and BET (Brunauer, Emmett, Teller) [13].

This work presents experimental results for adsorption capacities of N_2 and CO_2 on a commercial activated carbon by laboratory scale adsorption cell system. The obtained results are compared with literature. In the parametric study, the effect of pressure and temperature on capacity was examined experimentally in the adsorption cell system. Using the data obtained after experimental studies, Langmuir and Freundlich isotherm models and adsorption behavior were investigated and model parameters were determined and their physical meanings were explained.

2 Material and Method

In the experimental study, the effect of pressure and temperature on the equilibrium adsorption capacity of pure CO_2 and N_2 gases on commercial activated carbon was examined. Granular activated carbon in the particle size range of 0.6 mm-2.38 mm taken from DamlaNem Kimya Ltd. (Sincan, Ankara) was used as adsorbent. High purity N_2 (99.99%) and CO_2 (99.99%) gases taken from Samtaş A.Ş. were used as adsorbate gases. Pore size distribution and surface area of activated carbon were determined by characterization studies. In the experiments, equilibrium adsorption capacities were calculated by volumetric method. The experiments were carried out in the adsorption cell system. The pore properties of commercial activated carbon are presented in detail in Section 2.1, and the volumetric method and the adsorption cell system are presented in detail in Section 2.2.

2.1. Properties of activated carbon as an adsorbent

Granular commercial activated carbon with a particle size range of 0.6-2.38 mm was used in the experiments. BET analysis was performed on Quantochrome brand Autosorb-1 model N_2 adsorption-desorption device in order to determine particle size distribution, pore properties and surface area. N_2 adsorption/desorption isotherm is presented in Figure 1. The N_2 adsorption/desorption behavior of commercial activated carbon was found to be consistent with type IV adsorption isotherm. The hysterisis behavior seen at a relative pressure of about 0.4 is type H3. H3 type isotherms are generally observed in materials with narrow space and irregular pore

structure [14]. The Type IV behavior conforms to the adsorption isotherms, where the adsorption heat of the first layer is higher than the condensation temperature and where the capillary greatest. The occurrence of hysterisis is an indication that the isotherms of adsorption and desorption follow different pathways. This is explained by the emptying of narrow pores from wide pore openings at the surface. Generally, adsorption isotherms in micro- and mesoporous-containing solids conform to type IV [15].

The average pore diameter of BJH (Barret-Joiner-Halenda) and activated carbon is 10.1 nm and 3.7 nm for mesopores, while it was also determined that there are micropores of 1.3 nm size in the structure. The average pore size distribution results are given in Figure 2. The BET-specific surface area value is 868.8 m^2/g. The pore diameter was 1.194 nm and the pore volume was 0.4658 cm^3/g.
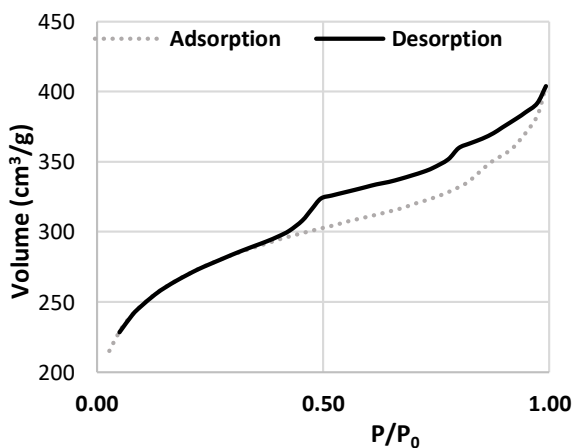
Fig 1. N$_2$ adsorption/desorption isotherm of commercial activated carbon
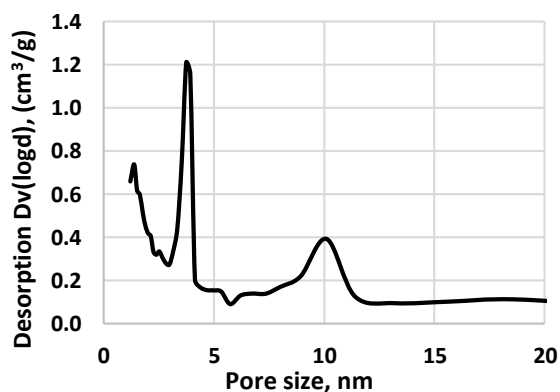
**Fig 2.** Average pore size distribution of commercial activated carbon

2.1. Volumetric method and adsorption cell system

In this study, the adsorption capacities of N$_2$ and CO$_2$ on a commercial activated carbon and the effect of pressure on the capacities were investigated by laboratory scale

adsorption cell system. Adsorption tests were performed at pressures ranging from 1 bar to 6 bar. In addition, operating temperatures were kept lower than room temperature with a range of 12°C-18°C.

Figure 3 presents a schematic representation of the adsorption cell system. The system has an adsorbent cell made of stainless steel. At the top of the cell, there is a gas inlet-outlet line and two valves for the opening and closing process. At the top of the gas outlet line, a Keller model Leo 2 model digital manometer (0.1 precision) is placed to read the internal pressure of the cell. On the left side of the adsorption cell there are cylinders for adsorbate gases. One GAST DOA-P504-BN model vacuum pump is connected to the output current line of the cell.

Volumetric method was used to determine adsorption capacities. In the volumetric method, the amount of gas remaining in the system at the end of the experiment is calculated by filling the adsorbate gas into the system and observing the pressure drop and subtracting the amount of gas remaining in the system at the end of the experiment.
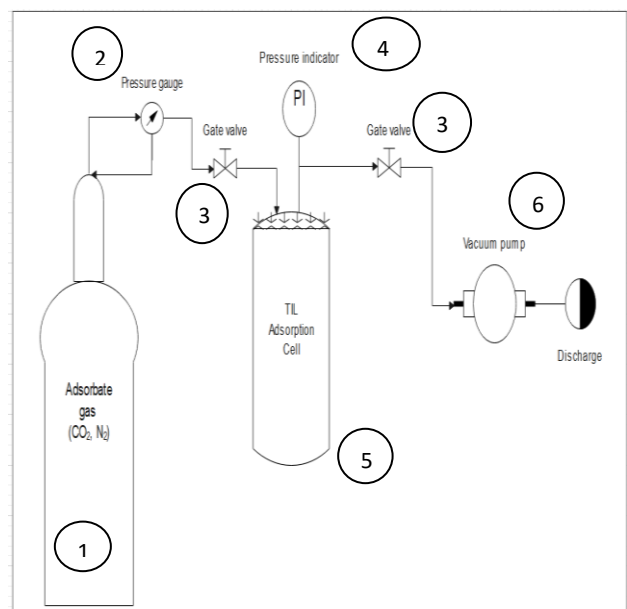
Fig 3. Schematic representation of the adsorption cell system (1-gas cylinder, 2-pressure gauge, 3-gate valve, 4- pressure indicator, 5- adsorption cell, 6- vacuum pump)

For this, it is necessary to first calculate how much volume the adsorbent will occupy inside the cell and the volume in which the gas can be found. All equations used in the volumetric method are from Eq.1 to Eq. 8.

The adsorption cell length is 14 cm and the diameter is 6.53 cm. The total volume considering the inlet and outlet pipes of the system (Eq. 1) was calculated as 549.3 cm^3 when the volume of cells and pipes was considered. Considering that the required amount of adsorbents filled into the cell, the volume of adsorbents in the cell was calculated with Eq. 2 using particle properties. When the cell is filled with an adsorbent, the volume in which the adsorbate gas can be found is called V$_{gas}$. Accordingly, the volume of gas was

found by subtracting from the total volume the volume occupied by the adsorbent. If the amount of the adsorbent to be used, particle density and void fraction are known, the volume in the cell can be calculated for each adsorbent.

$$V_{total} = D^2_{cell} L_{cell} + D^2_{pipe} L_{pipe} \quad (1)$$

$$V_{ads} = m_{ads} / (1-\varepsilon)\rho_p \quad (2)$$

$$V_{gas} = V_{total} - V_{ads} \quad (3)$$

Since experiments were carried out at values higher than atmospheric pressure in determining adsorption capacities, the behavior of gases must be taken into account as the actual gas behavior. For this, the compressibility factor of the gases (Eq. 4) was determined according to the operating temperature and pressure. At the beginning of the experiments the moles of the gas in the cell was calculated using Eq. 5. After the system comes to equilibrium the mole of the gas in the cell was calculated with Eq. 6. The difference between the total amount of adsorbed gas hence was calculated with Eq. 7. Equilibrium adsorption value was defined in Eq. 8.

If the gas pressure in the first state fed to the cell was P_1 and , the moles of the gas in the 1st state was calculated with Eq. 5. The pressure value after the system comes to equilibrium is called P_2 and the mole of the gas in the 2nd state was calculated with Eq. 6. It is the difference between the total amount of adsorbed gas and the mole amounts in the system in the 1st and 2nd states, it was calculated with Eq.7. Equilibrium adsorption value is defined as the amount of gas that 1gram adsorbent substance can adsorb. It was calculated with Eq. 8.

$$Z = Z (P_r, T_r) = (PV)/(nRT) \quad (4)$$

$$n_1 = (P_1 V_{gas})/(ZRT) \quad (5)$$

$$n_2 = (P_2 V_{gas})/(ZRT) \quad (6)$$

$$n_{adsorbed} = n_1 - n_2 \quad (7)$$

$$n_{adsorbed,eq} = n_{adsorbed\ gas} / \text{gram adsorbent} \quad (8)$$

The adsorbent (activated carbon) whose capacity was going to be determined was dried in an oven at 95 °C for 2.5 hours beforehand. It was kept in a desiccator for testing. In the beginning of the experiment, the adsorbent was quickly filled into the cell so that its contact with air was kept minimal. After making sure that the adsorbent bed was equal everywhere in the cell, the cover of the cell was closed. Then, it was vacuumed with the help of the vacuum pump connected to the output stream and the pressure in the system was provided to be -0.7 bar. After the vacuum, the gas was filled to the cell and pressure drop in the system was observed with time. When the system pressure had reached equilibrium, the experiment was ended.

3 Results and Discussion

As a result of the experimental study, the effect of pressure and temperature on the adsorption of CO_2 and N_2 on commercial activated carbon was compared with the literature studies and presented in Sections 3.1 and 3.2. With the experimental data obtained, Langmuir and Freundlich isotherm models were obtained and the model parameters were determined. The theoretical assumptions of the models and the physical outputs of the model parameters for the adsorption process are described in Section 3.3.

3.1. N_2 adsorption results

In N_2 adsorption experiments, experiments were carried out at 1 bar working pressure and at different temperatures. The N_2 adsorption capacity of activated carbon at 18°C was determined as 0.31 mmol N_2/g AC. In adsorption studies carried out under room temperature conditions, the N_2 adsorption capacity of various activated carbons was reported as approximately 0.3 mmol N_2/g AC [2, 16-18]. The result obtained at 18 °C was found to be in good agreement with the literature. At a constant adsorption pressure of 1 bar, the N_2 adsorption capacity increased as the temperature was decreased. The N_2 capacity at 15°C was calculated as 0.31 mmol N_2/g AC, at 14°C the N_2 capacity was 0.32 mmol N_2/g AC, and at 13°C the N_2 capacity was calculated as 0.42 mmol N_2/g AC. In the study of Qu et al., the adsorption capacity for 1 bar-10 °C is 0.65 mmol N_2/g AC [19]. Considering the low temperature effect in the study, it is expected that the capacity is larger than the capacity at 13°C, 14°C and 15°C, but it also supports that the adsorption takes place physically [20-24]. In Figure 4, the relationship between the N_2 adsorption capacities of activated carbon and temperature is given.
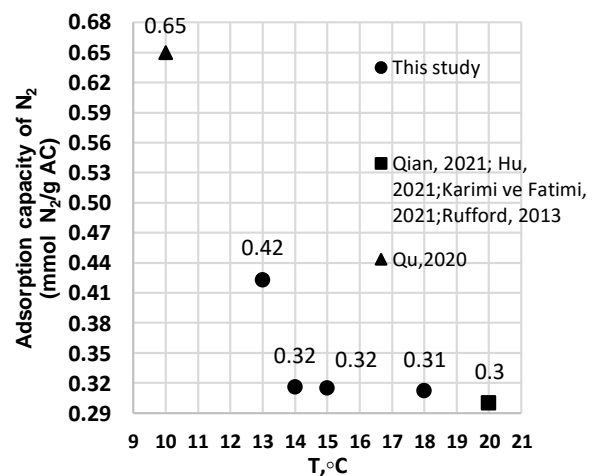
Fig 4. Change of the adsorption capacity of activated carbon N_2 with temperature (@ 1bar)

In the adsorption experiments carried out at 2 bar and 14 °C, the N_2 adsorption capacity of activated carbon was determined as 0.7 mmol N_2/g AC. In the study of Qian et al., the N_2 adsorption capacity at 2 bar pressure and 25°C is 0.6 mmol N_2/g AC, and at 5°C the adsorption capacity is 0.81 mmol N_2/g AC [17].
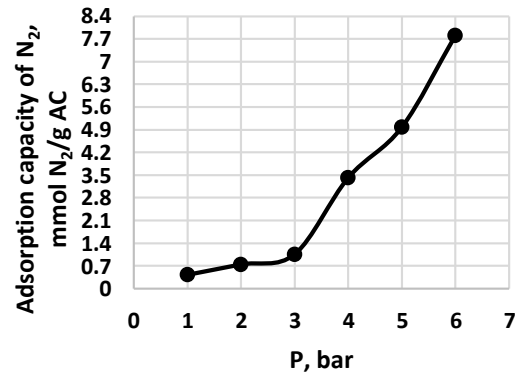
Likewise, in the study of Wu et al., the N_2 adsorption capacity on activated carbon was stated as 0.6 mmol N_2/g AC for 2 bar-20°C [21]. Accordingly, the adsorption capacity at 14°C was higher (>0.6 mmol N_2/g AC) than the adsorption capacity at 25°C, but also lower as expected at a low temperature of 5°C. Low temperature values affect the capacity positively because the physical adsorption is an exothermic process [20, 21].

In the adsorption experiments carried out at 3 bar and 14 °C, the N_2 adsorption capacity of activated carbon was determined as 1.1 mmol N_2/g AC. In the adsorption experiments carried out at 4 bar and 14 °C, the N_2 adsorption capacity of activated carbon was determined as 3.4 mmol N_2/g AC. In the studies of Wu et al. (2015) and Qian et al. (2021), the N_2 adsorption capacity was stated as 0.7 and 0.8 mmol N_2/g AC, respectively, in experiments at 3 bar-20°C [21]. With the effect of low temperature, its capacity at 14°C is higher than 0.8 mmol N_2/g AC. In the study of Qu et al. (2020), the N_2 capacity is 1.1 mmol N_2/g AC at 3 bar-10°C and 0.85 mmol N_2/g AC at 25°C [19]. Accordingly, the capacity of 1.1 mmol N_2/g AC and 3.4 mmol N_2/g AC was found to be compatible with the literature, considering that for 14°C it is close to 10°C and yet the pressure is higher.

In the adsorption experiments carried out at 4 bar and 5 bar (14 °C), the N_2 adsorption capacities of activated carbon were determined as 3.4 mmol N_2/g AC and 4.9 mmol N_2/g AC, respectively. In the adsorption experiments carried out at 6 bar and 14 °C, the N_2 adsorption capacity of activated carbon was determined as 7.8 mmol N_2/g AC. In the study of Park et al., the adsorption capacity was specified as 1.3 and 1.5 bar, respectively, at 20°C -5 and 6 bar. Considering that the temperature is quite low in the experimental study, it is expected that the capacity value will be higher [25]. As the working pressure increases, the adsorption capacity of N_2 on activated carbon increases (Figure 5). The relationship of adsorption capacity with pressure is in good agreement with the literature [2, 16, 26-28]. The results of the N_2 adsorption capacities on activated carbon are presented in Table 1.

Table 1. N_2 adsorption capacities (@ 14°C)

| P_1, bar	$P_{equilibrium}$, bar	n_{ads}, mmol/g
1	0.6	0.4
2	1.3	0.7
3	2	1.1
4	2.5	3.4
5	2.8	4.9
6	2.5	7.8

Fig 5. Effect of pressure on N_2 adsorption capacity (@14°C)

3.2. CO_2 adsorption results

In the adsorption experiments carried out at 1 bar and 14 °C, the CO_2 adsorption capacity of activated carbon was determined as 2.7 mmol CO_2/g. In Fan (2016) and Wu (2015) studies, the CO_2 capacity of Norit is 2.27 mmol CO_2/g Norit (1 bar-@25°C) and the CO_2 capacity of activated carbon is 2.5 mmol CO_2/g Norit (1 bar-@20°C), respectively. [21, 29]. Likewise, when the literature studies and 1 bar test results are compared, the CO_2 adsorption capacity of activated carbon is above 2 mmol CO_2/g AC as expected.

In Figure 6, the relationship between the CO_2 adsorption capacities of activated carbon and temperature is given. When the capacity value of the adsorption carried out at 14°C is compared with the findings in the literature, it is seen that the capacity is higher at temperatures lower than room temperature compared to the values reported at higher temperatures. In studies on activated carbons in the literature, it has been observed that the CO_2 capacity decreases at high temperatures. This is due to the exothermic nature of the adsorption process. In the exothermic process, the molecular diffusion rate and surface adsorption energy increase with increasing temperature, leading to the possibility of chemical adsorption rather than physical adsorption [30-32].
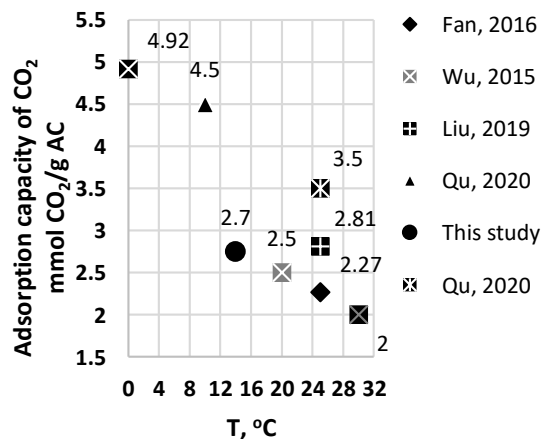
Fig 6. Change of the CO_2 adsorption capacity of activated carbon with temperature (@ 1bar)

In the adsorption experiments carried out at 2 bar and 14 °C, the CO_2 adsorption capacity of activated carbon was determined as 3.1 mmol CO_2/g AC. In the experiments carried out at 3 bar in Fan (2016) and Wu (2015) studies, the CO_2 adsorption capacity was stated as 3 mmol CO_2/g AC [21, 29]. In the adsorption experiments carried out at 3 bar and 14 °C, the CO_2 adsorption capacity of activated carbon was determined as 3.6 mmol CO_2/g AC. In the literature, the CO_2 adsorption capacity at room temperature and 3 bar conditions is reported to be about 4 mmol CO_2/g AC [21, 29]. Experiment results were expected to be close to 4 mmol CO_2/g AC, yet a maximum of 3.6 mmol CO_2/g AC CO_2 was adsorbed. The slight difference between the experimental results and the literature may be due to the differences in the organic bonds and functional groups that the activated carbon samples naturally contain.

In the adsorption experiments carried out at 4 bar and 14 °C, the CO_2 adsorption capacity of activated carbon was determined as 4.6 mmol CO_2/g AC. In the literature, the CO_2 adsorption capacity at room temperature and 4 bar conditions is approximately 4-5 mmol CO_2/g AC [21, 29]. In the adsorption experiments carried out at 5 bar and 14 °C, the CO_2 adsorption capacity of activated carbon was determined as 6.2 mmol CO_2/g AC. In the literature, the CO_2 capacity of activated carbon at room temperature and 5 bar conditions has been reported as 5.2 mmol CO_2/g AC [25]. In the adsorption experiments carried out at 6 bar and 14 °C, the CO_2 adsorption capacity of activated carbon was determined as 7.4 mmol CO_2/g AC. The results obtained at 5 bar and 6 bar are higher than the reported values in literature due to temperature difference (this study:14°C, literature value: room temperature). As the working pressure increases, the CO_2 adsorption capacity on the activated carbon increases (Figure 7). The results of CO_2 adsorption capacities on activated carbon are presented in Table 2.

Table 2. CO_2 adsorption capacities (@14°C)

P_1, bar	$P_{equilibrium}$, bar	n_{ads}, mmol/g
1	0.4	2.7
2	0.6	3.1
3	1.4	3.6
4	1.9	4.6
5	2.2	6.2
6	2.7	7.4

Basically, the important point in the separation of N_2-CO_2 containing streams by the adsorption process is the surface properties of the selected adsorbent. Different dipole-quadrupole forces and molecular polarization energies of gas molecules affect the adsorption process. The fact that the adsorbent surface is more heterogeneous for CO_2 adsorption and the presence of various ions and functional groups in the adsorbent structure increases the interaction of the molecule with the surface [33, 34]. Besides, the polarizability of the CO_2 molecule is higher than that of the N_2 gas (Table 3). This is one of the important features that increase the interaction of the CO_2 molecule with the surface. Therefore, increased surface interaction due to surface heterogeneity and high polarizability allows the CO_2 adsorbent capacity to increase [35-37]. The molecular properties of CO_2 and N_2 are given in Table 3.
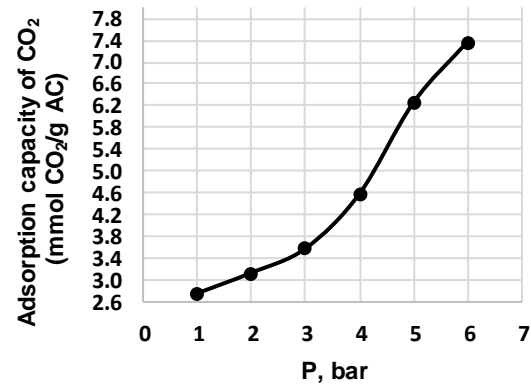
Fig 7. Effect of pressure on CO_2 adsorption capacity (@14°C)

Table 3. Molecular properties of N_2 and CO_2 [21]

Gas	Kinetic molecular diameter, nm	Quadripole moment 10^{-40}, cm^2	Polarizability 10^{-25}, cm^3	Dipole moment
CO_2	0.33	-137	29.1	0
N_2	0.36	-4.9	17.4	0

The kinetic diameter of gas molecules is also important for separation with adsorption. Kinetic diameters of the molecules are CO_2:0.33 nm; N_2:0.364nm; CH_4:0.38 nm; H_2O:0.265nm; O_2: 0.346 nm; in the presence of SO_2 (0.360 nm) in the gas stream, the adsorption precedence was observed as $H_2O<CO_2<O_2<SO_2<N_2<CH_4$ [38-40]. The molecular diameter of CO_2 is 0.33 nm, which is considerably smaller than the molecular diameter of N_2. Considering the very high surface area and pore volume of activated carbons, the probability of small-scale CO_2 molecules penetrating into the pores is also high [41]. The relatively small molecular diameter of CO_2 leads to its high adsorption capacity.

3.3. Modeling of Langmuir and Freundlich Isotherms

The Langmuir isotherm model is used to describe equilibrium adsorption conditions, especially gas-solid interaction of adsorbent materials. The Langmuir model is based on some assumptions about the adsorption mechanism. These assumptions are that the entire surface of the adsorbent is homogeneous, all active sites of the adsorbent have equal energy and their distribution on the material is homogeneous, the adsorption energy is

constant, monolayer adsorption is explained, and there is no interaction between the adsorbate molecules [13, 36, 42]. Langmuir model is expressed in Eq.9. Where Θ is fractional coverage; q is the amount adsorbed; q_m is the maximum adsorption capacity; B is called as affinity constant and it describes the ratio of the adsorption rate and desorption rate; P is the pressure [13, 43]. Langmuir model can be linearized like in Eq. 10.

$$\Theta = q/q_m = (BP)/(1+BP) \qquad (9)$$

$$P_e/q = P_e/q_m + 1/Bq_m \qquad (10)$$

The Freundlich isotherm model is widely used in adsorption, presenting the physical and multilayer adsorption process (Eq. 11). Also, it is an empirical equation. k and n are Freundlich constant parameters. q is the amount adsorbed and P is the pressure [13]. The Freundlich isotherm model can also be linearized. Linear model is presented in Eq. 12. Langmuir and Freundlich model parameters of CO_2 and N_2 adsorption in experiments with activated carbon are presented in Table 4. By using the experimental data on the adsorption of both gases, their compatibility with the linear model equations was investigated.

$$q = kP^{1/n} \qquad (11)$$

$$\log(q) = \log(k) + (1/n)\log(P) \qquad (12)$$

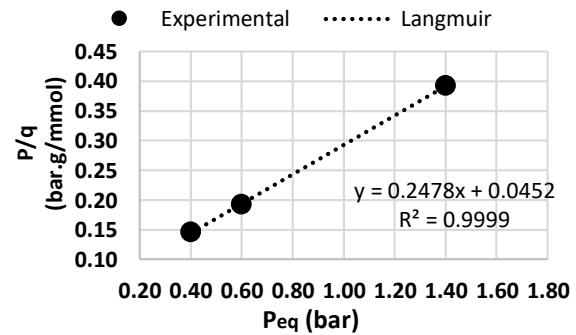**Table 4.** Langmuir ve Freundlich isotherm model parameters

Langmuir isotherm model				Freundlich isotherm model			
CO_2		N_2		CO_2		N_2	
q_m	B	q_m	B	k	n	k	n
4.04	5.48	2.98	0.27	1.63	1.23	1.01	1.09

*(q_m, mmol gas/g adsorbent ; B, bar^{-1})

Langmuir model affinity constants (B) were calculated as 5.48 bar^{-1} for CO_2 gas and 0.27 bar^{-1} for N_2 gas. The affinity constant is an indicator of how strongly the adsorbate molecules will adhere to the surface. When B>1, it is stated that the adsorption rate is higher than the desorption rate [44]. It has been observed that the affinity constant for the CO_2 gas to be adsorbed on the activated carbon is higher than the N_2 gas. This supports the fact that the CO_2 capacity of activated carbon is higher than the N_2 capacity even at low pressures.

With the Langmuir isotherm model, the experimental data were compatible with the capacities at 1, 2 and 3 bar pressure values. Non-ideal conditions in isotherms are usually due to the heterogeneity of the adsorbent surface. Such heterogeneities are generally observed when using activated carbon [45]. Langmuir model graphs created for CO_2 and N_2 adsorption are presented in Figure 8 and Figure 9, respectively. At low pressures, the experimental data showed a better fit with the Langmuir model, and deviations in the isotherm

occurred at values higher than 3 bar pressure. At low adsorption pressures, the filling in the micropores takes place in a single layer. In high pressure adsorption, the probability of multi-layer filling in the pores instead of a single layer is very high. Another experimental result supporting the possibility of multilayer adsorption on activated carbon was observed for CO_2 adsorption in the Freundlich model.

Fig 8. Fit of the Langmuir model and experimental data for CO_2 adsorption
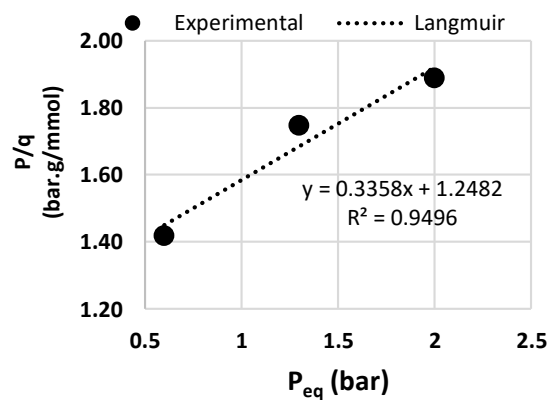

**Fig 9.** Fit of the Langmuir model and experimental data for N_2 adsorption

In the Freundlich isotherm model, the parameter k is an indicator of whether the adsorption in the process is more physical or chemical. Larger k values indicate greater physisorption compared to chemisorption [45-47]. In the adsorption of CO_2 and N_2 gases, the k values were determined as 1.63 and 1.01, respectively. Although it is known that the polarizability and quadripole moment of CO_2 molecules are higher compared to N_2 (Table 3), the k value of CO_2 adsorption was also found to be higher than the k value of N_2 adsorption. CO_2 molecules are better adsorbed on the activated carbon surface due to the higher electrical field. High k value and high electrical field properties are in good agreement with each other in CO_2 adsorption.

The Freundlich isotherm has no Henry's law behavior at low pressures and a finite limit when pressure is high. It can be applied in gas phase systems with heterogeneous surfaces, provided that the pressure range is not too wide. It is generally valid in the narrow range of adsorption data. It has been stated that since it cannot be applied in the entire pressure range, it is

possible to choose and limit the data [42]. Since the behavior at low pressures is not compatible, data at 1 bar pressure were not used in the creation of the Freundlich model. The data on CO_2 and N_2 adsorption and Freundlich isotherm model compatibility are presented in Figure 10 and Figure 11. The agreement of CO_2 adsorption with the Freundlich model is quite high, but the model agreement for N_2 adsorption R^2 value remained at 0.796. While other values except for 1 bar pressure in CO_2 adsorption values are compatible with the model, in N_2 experiments, the model can show compatibility only with values in a certain operating range of 4, 5 and 6 bar.
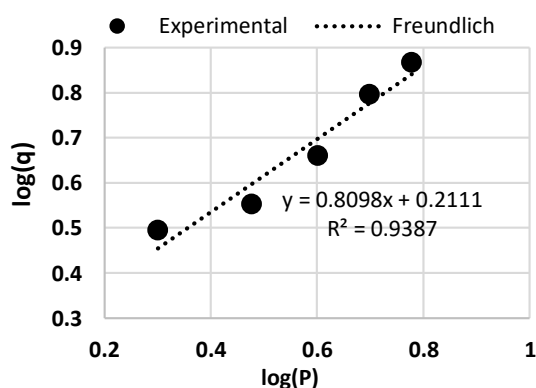
Fig 10. Fit of Freundlich model and experimental data for CO_2 adsorption
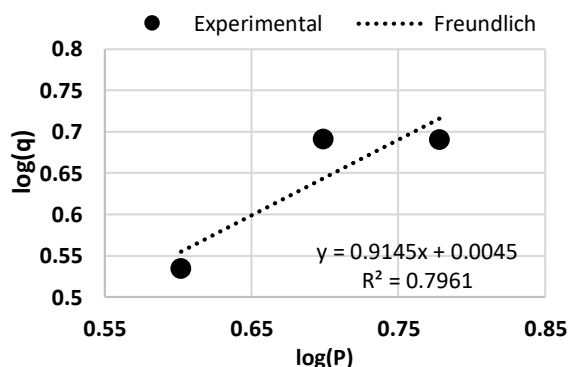
Fig 11. Fit of Freundlich model and experimental data for N_2 adsorption

The Freundlich model showed better agreement with the experimental data at high pressures. Since this model can define multilayer adsorption, the model created for CO_2 (Figure 10) has been studied with 5 experimental data. Thus, it is stated that multilayer adsorption can take place on activated carbon compared to monolayer adsorption. This also helps in explaining the way and the order in which the pores are filled in the pore size distribution and adsorption. The filling of pores in activated carbons or activated carbon fibers begins with the filling of micropores. Then, a multi-layered film is formed on the mesopore walls, and finally, the empty spaces inside the mesopores are filled by capillary condensation. There are two stages in filling the micropores. In the first stage, the sizes are similar to the diameters of adsorbent molecules and are

the dominant mechanism for smaller micropores. This process is due to the overlap of the plane surface energy corresponding to the gas-solid interaction energy and the potential fields originating from the neighbour walls of the pore. In the second step, the adsorbed gas molecules prefer to combine with other previously adsorbed molecules rather than completing a monolayer through interaction with the pore walls [48].

4 Conclusion

The aim of the study was to find a high capacity and cheaper adsorbent alternative to PSA systems, which are suitable technologies for the capture and purification of coal bed methane stream. In the study, the equilibrium adsorption capacities of CO_2 and N_2 gases of a commercial activated carbon were investigated in a laboratory scale cell adsorption system. It was seen that as the adsorption pressure was increased, the equilibrium adsorption capacity increased. In experiments carried out at different temperatures, it was observed that low adsorption temperatures positively affected the adsorption capacity. This showed that CO_2 and N_2 gases were adsorbed on activated carbon by physical adsorption. Besides, it was stated that single-layer adsorption in the low pressure region could be defined with the Langmuir model and multi-layer adsorption could be defined with the help of the Freundlich model as the pressure increases. The capture and purification of coal bed methane, which is an important source of CO_2 and CH_4 emissions, offers an alternative approach to today's energy and greenhouse gas problems. The design of pressure swing adsorption systems (PSA) for the capture and purification of coal bed methane and the development of suitable adsorbents for these systems are extremely important. This concept candidates to ensure national energy security.

References

1. Recent Daily Average CO_2 at Mauna Loa, https://www.co2.earth/daily-co2#:~:text=419.88%20ppm&text=Units%20%3D%20parts%20per%20million%20(ppm). [Accessed 19.02.2023]

2. K. Karimi, S. Fatemi., J.Environ. Chem. Eng. **9,** 5 (2021).

3. H. Moradi, H. Azizpour, H. Bahmanyar, N. Rezamandi, P. Zahedi. Chem. Eng. Technol. **44**, 7 (2021)

4. W. Roman, G. Xiao, A. Islam, E. F. May. J. Chem. Eng. Data. **392**, 123753 (2020)

5. C. Wan, X. Gou, E. Zou, M. Luo, M. Chen, M. Yang, H. li C. jia, C. Deng, C. Sun, B. Liu, L. Yang, G. Chen. GEE. **5**, 3 (2020)

6. Q. Zhu. Natural Gas Industry. **9**, 5 (2022)

7. S. Neishabori, S. Sharifnia, F. Rahimpour.j. Nat. Gas Eng. **54**, 37-46 (2018)

8. A.A . Abd, M.R. Othman, I. K. Shamsudin, Z. Helwani, I. Idris. Chem. Eng. J. **453**, 139774 (2023)

9. M.H.V. Bahrun, A. Bono, N. Othman, M.A.A. Zaini. Chem. Eng. Res. Des. **183**, 285-306 (2022)

10. N.H. Sabri, N.H.A. Rani, N.F. Mohamad, N.A.S. Mohd Muhsen, M.S. Md Zaini. Mater Today. (2023)

11. Z. Bicil. Karbon Içerikli Malzemelerin Hazırlanması Ve Gaz Depolama Özelliklerinin Incelenmesi. Master of Thesis, Balıkesir Üniversitesi, (2021)

12. R. Javani, H. Maghsoudi, S. D. Gilan, M. Majidpour. Se. Sci. Technol. **56**, 2562-2577 (2021)

13. J. Wang, X. Guo. Chemosphere **258**,127279 (2020)

14. S. Lowell, J. Shield. *Powder Surface Area and Porosity*. 2 ed. New York: Chapman and Hall, (1984)

15. S. Bal. Isıl İşlem Görmüş Kömürlere Mtbe'nin Adsorpsiyonu. Master of Thesis, Ankara Üniversitesi (2007)

16. G. Hu, Q. Zhao, L. Tao, P. Xiao, P.A. Webley. Chem. Eng. Sci. **229**, 116152 (2021)

17. Z. Qian,Y. Yang, P. Li, J. Wang, A.E. Rodrigues. Chem. Eng. J. **419**, 129657.

18. T.E. Rufford, G.C.Y. Watson, T.L. Saleman, P.S. Hofman, N.K. Jensen, E. F. May. Ind. Eng. Chem. Res. **52**,14270-81 (2013)

19. D. Qu, Y. Yang, Z. Qian, P. Li, J. Yu, A.M. Ribeiro, A.E. Rodrigues. Chem. Eng. J. **380**, 122509.

20. E. Kurtaran. Sepiolit Ile Sulu Çözeltilerden Ni(Ii) İyonunun Giderilmesi. Master of Thesis, Eskişehir Osmangazi Üniversitesi (2013)

21. Y. Wu, Y. Yang, X.M. Kong, P. Li, J. G. Yu, A. M. Ribeiro, A.E. Rodrigues. J. Chem. Eng. Data. **60**, 9 (2015)

22. E. Yörükoğulları, Anadolu Üniversitesi Fen Fakültesi Yayınları, 58 (1997)

23. S. Dikmen. Hdtma-Zeolitin Hazırlanması Ve Sulu Çözeltiden Nitrat Adsorpsiyonu. PhD Thesis. Anadolu Üniversitesi, (2007)

24. M. Kılıç. Kurşun (II) Ve Cıva (II) İyonlarının Biyokütle Üzerine Adsorpsiyonunun İncelenmesi. PhD Thesis, Süleyman Demirel Üniversitesi (2004)

25. Y. Park, D. Moon, Y. Kim, H. Ahn, C. Lee. Adsorption, **20**, 4 (2014)

26. N. Tzabar, H.J. Holland, C.H. Vermeer, H.J.M. ter Brake. IOP Conference Series: Materials Science and Engineering. **101**, 012169

27. L. Li, J. Yang, J. Li, Y. Chen, J. Li. Micropor. Mesopor. Mat.**198**. 236-46 (2014)

28. Y. Li, R. Xu, B. Wang, J. Wei, L: Wang, M. Shen, J. Yang. Nanomaterials **9**, 266 (2019)

29. W. Fan, A. Chakraborty, S. Kayal. Energy **102**, 491-501 (2016)

30. M. Marato-Valer, M. Mercedes, Z. Tang, Y. Zhang. FPT. **86**, 1487-502 (2005)

31. M. S. Shafeeyan, W.M.A. Wan Daud, A. Houshmand, A. Arami-Niya. Appl. Surf. Sci. **257,** 3936-42 (2011)

32. P. Ning, F. li, H. yi, X. Tang, J. Peng, Y. Li, Dan He, H. Deng.Sep. Purif. Technol. **98,** 321-26 (2012)

33. M.S. Shafeeyan, W.M.A.Wan Daud, A. Houshmand, A. Shamiri. JAAP. **89,** 143-51 (2010)

34. C. Pevida, M.G. Plaza, B. Arias, J. Dermoso, F. Rubiera, J. Pis. Appl. Surf. Sci. **254**,7165-72 (2008)

35. A.J. Huth, J.M. Stueve, V. V. Guliants J. Membr. Sci. **403-404,** 236-49 (2012)

36. D.A. Kennedy, M. Mujcin, E. Trudeau, F. H. Tezel. J. Chem. Eng. Data. **61.** 3163-76 (2016)

37. X. Xu, X. Zhao, L. Sun, X. Liu. Journal of Natural Gas Chemistry **17**, 391-96 (2008)

38. G. Aguilar-Armenta, M.E. Patino-Iglesias, R. Leyva-Ramos. Adsorp. Sci. Technol. **21**, 81-91 (2003)

39. A.F. Ismail, K. Khulbe, T. Matsuura. Gas Separation Membranes. 1 ed.: Springer International Publishing, (2015)

40. D.W. Breck. Zeolite Molecular Sieves: *Structure, Chemistry*, and Use. New York: Wiley (1974)

41. T. L. P. Dantas, F. M. T. Luna, I. J. Silva, D. C.S. de Azevedo, C. A. Grande, A.E. Rodrigues, R.F.P.M. Moreira. Chem. Eng. J. **169,** 11-19 (2011)

42. D.D. Do. Adsorption Analysis*: Equilibria and Kinetics*. London: Imperial Collage (1998)

43. P. Li, F. H. Tezel. J. Chem. Eng. Data. **4**, 8-15 (2009)

44. W.L. McCabe, J.C. smith, P. Harriot. *Unit Operations of Chemical Engineering*. 7. ed. Singapore: McGraw Hill (2005)

45. M.S. Shafeeyan, W.M.A.Wan Daud. Chem. Eng. Res. Des.**104**, 42-52 (2015)

46. V. Ferraro, I.B. Cruz, R.F. Jorge, M.E. Pintado, P.M.L. Castro. J. Chem. Eng. Data. **58**, 707-17 (2013)

47. M.D. LeVan, G. Carta, C.M. Yon. Energy **16,** 17 (1997)

48. M.A. Hernandez, F. rojas, V.H. Lara. J. Porous Mater. **7,** 443-54 (2000)

Authors' background

Your Name	Title*	Research Field	Personal website
Duygu UYSAL	Associate Professor	Mass Transfer, Heat Transfer, Energy, Transport Phenomena, Separation Processes, Fluidized beds	https://avesis.gazi.edu.tr/duysal
Hazal OZTAN	Research and Teaching Assistant (MSc)	Energy, Separation Processes, Engineering and Technology, Gasification, Fluidized Beds	https://avesis.gazi.edu.tr/hazaloztan